Environmental Research 160 (2018) 195–202

Contents lists available at ScienceDirect

Environmental Research

journal homepage: www.elsevier.com/locate/envres

Excess Lead-210 and Plutonium-239 + 240: Two suitable radiogenic soil erosion tracers for mountain grassland sites

K. Meusburger[a,*], P. Porto[b], L. Mabit[c], C. La Spada[b], L. Arata[a], C. Alewell[a]

[a] Environmental Geosciences, University of Basel, Bernoullistrasse 30, CH-4056 Basel, Switzerland
[b] Dipartimento di AGRARIA, Università degli Studi Mediterranea di Reggio Calabria, Italy
[c] Soil and Water Management and Crop Nutrition Laboratory, FAO/IAEA Agriculture & Biotechnology Laboratory, IAEA Laboratories Seibersdorf, Seibersdorf, Austria

ARTICLE INFO

Keywords:
$^{210}Pb_{ex}$
$^{239+240}Pu$
^{137}Cs
Fallout radionuclide
Chernobyl
Soil erosion
Land use change

ABSTRACT

The expected growing population and challenges associated with globalisation will increase local food and feed demands and enhance the pressure on local and regional upland soil resources. In light of these potential future developments it is necessary to define sustainable land use and tolerable soil loss rates with methods applicable and adapted to mountainous areas. Fallout-radionuclides (FRNs) are proven techniques to increase our knowledge about the status and resilience of agro-ecosystems. However, the use of the Caesium-137 (^{137}Cs) method is complicated in the European Alps due to its heterogeneous input and the timing of the Chernobyl fallout, which occurred during a few single rain events on partly snow covered ground. Other radioisotopic techniques have been proposed to overcome these limitations. The objective of this study is to evaluate the suitability of excess Lead-210 ($^{210}Pb_{ex}$) and Plutonium-239 + 240 ($^{239+240}Pu$) as soil erosion tracers for three different grassland management types at the steep slopes (slope angles between 35 and 38°) located in the Central Swiss Alps. All three FRNs identified pastures as having the highest mean (± standard deviation) net soil loss of −6.7 ± 1.1, −9.8 ± 6.8 and −7.0 ± 5.2 Mg ha^{-1} yr^{-1} for ^{137}Cs, $^{210}Pb_{ex}$ and $^{239+240}Pu$, respectively. A mean soil loss of −5.7 ± 1.5, −5.2 ± 1.5 and-5.6 ± 2.1 was assessed for hayfields and the lowest rates were established for pastures with dwarf-shrubs (−5.2 ± 2.5, −4.5 ± 2.5 and −3.3 ± 2.4 Mg ha^{-1} yr^{-1} for ^{137}Cs, $^{210}Pb_{ex}$ and $^{239+240}Pu$, respectively). These rates, evaluated at sites with an elevated soil erosion risk exceed the respective soil production rates. Among the three FRN methods used, $^{239+240}Pu$ appears as the most promising tracer in terms of measurement uncertainty and reduced small scale variability (CV of 13%). Despite a higher level of uncertainty, $^{210}Pb_{ex}$ produced comparable results, with a wide range of erosion rates sensitive to changes in grassland management. $^{210}Pb_{ex}$ can then be as well considered as a suitable soil tracer to investigate alpine agroecosystems.

1. Introduction

Land degradation and especially soil erosion are associated with the irretrievable loss of the basic soil resource and particularly in upland mountain areas have severe impacts on water storage and quality, entailing changes in water availability far beyond the mountain areas. In terms of food and feed resources, the importance of this relative unproductive marginal agricultural land decreased during the last 30 years due to the liberalization of agricultural markets that has promoted a global competition. In such a globalized market, farming in mountain regions is clearly disadvantaged because of higher production costs (Streifeneder and Rufjini, 2007) and, as a consequence, mountain farmland is abandoned in Europe (Lasanta et al., 2017). For example in Switzerland, despite subsidies, the number of farms decreased by 40% between 1985 and 2008 (BFS, 2009).

These mountain grasslands might, however, regain some of their importance because of the global demand for primary phytomass for food, which should be at least more than doubled by 2050 (Koning et al., 2008). The growing world population in combination with an unrestrained soil degradation (Borrelli et al., n.d) might increase food and feed shortage in future and trigger the expansion of cultivated land towards these grass- and woodlands (Fischer et al., 2011). In light of these future developments and the expected most pronounced effects of climate change impacting mountainous areas (Beniston, 2003, 2006; Meusburger et al., 2012), it is necessary to identify sustainable land management strategies and to characterize tolerable soil loss rates with specific techniques adapted to steep, inaccessible and rough climate conditions of mountain areas. Particularly snow and avalanches, acting

* Corresponding author.
E-mail addresses: Katrin.Meusburger@unibas.ch (K. Meusburger), L.Mabit@iaea.org (L. Mabit).

http://dx.doi.org/10.1016/j.envres.2017.09.020
Received 5 May 2017; Received in revised form 18 September 2017; Accepted 18 September 2017

as soil erosion agents themselves, greatly impede the use of traditional long-term soil erosion monitoring techniques such as sediment traps or erosion pins (Alewell et al., 2008; Konz et al., 2012; Meusburger et al., 2014).

Fallout radionuclides (FRN) are one of the most convenient approaches to quantify soil erosion in Alpine grasslands (Alewell et al., 2014), because they account for soil loss not only by water, but also for topsoil abrasion caused by snow movement in winter when conventional measurements are not feasible (Meusburger et al., 2014). Moreover, the FRN technique allows to complement and underpin modelled long-term soil erosion rates (Meusburger et al., 2010), although applications of FRNs in context of large scale model applications (e.g. Panagos et al., 2015) are still missing. When FRNs reach the soil surface by wet deposition, they are tightly adsorbed to fine soil particles and the subsequent lateral redistribution of adsorbed FRNs is mainly associated with soil redistribution (Zapata, 2002). The use of FRN measurements to quantify soil redistribution magnitude is commonly based upon a comparison of FRN inventories for individual sampling points to the local reference inventory, where soil erosion is indicated by lower FRN inventories, and sedimentation, by higher FRN levels as compared to the reference site (Ritchie and McHenry, 1990; Mabit et al., 2008).

The FRN Caesium-137 (^{137}Cs) is the most commonly used tracer for soil erosion assessment. This radioisotope was introduced into the global environment by the thermonuclear weapons testing that took place from the mid-1950s to the early 1960s and from nuclear power plant (NPP) accidents such as Chernobyl in April-May 1986. However, due to radioactive decay the concentrations of ^{137}Cs are decreasing particularly in the southern hemisphere, where ^{137}Cs fallout has been much lower than in the north hemisphere (where most of the nuclear tests took place). In addition, in the Swiss alpine areas, we are confronted with an unusually high heterogeneity of ^{137}Cs reference inventories (Alewell et al., 2014). The latter might be due to the highly uneven spatial distribution of the Chernobyl ^{137}Cs fallout and the partial presence of snow cover at the end of April-May 1986 that most likely enhanced heterogeneous redistribution during the snow melt process. This heterogeneity can complicate or even compromise the use of the ^{137}Cs method as the key assumption of homogeneity of the initial fallout is not fulfilled (Haugen, 1991; Lettner et al., 1999; Golosov et al., 2008, 2013; Mabit et al., 2013). The Chernobyl fallout entails a second limitation. To convert FRN inventories into yearly soil erosion rates, the proportion of ^{137}Cs Chernobyl fallout is required to refer the erosion rates to the correct time period.

To overcome these limitations associated with the use of ^{137}Cs in mountain areas, anthropogenic Plutonium-239 + 240 ($^{239+240}$Pu) has been suggested by the research community as a new radioisotopic approach to determine soil erosion rates in mountain areas (Alewell et al., 2014; Meusburger et al., 2016). Pu isotopes (i.e. ^{239}Pu [half-life = 24,110 years] and ^{240}Pu [half-life = 6561 years]) in European alpine areas originate solely from the past nuclear weapon tests, which resulted in a more homogenous input due to the longer fallout period above one decade (Alewell et al., 2014). Plutonium isotopes may also help to overcome the second limitation - the apportionment of the ^{137}Cs originating from Chernobyl fallout - by utilizing specific $^{239+240}$Pu/^{137}Cs activity ratios. Indeed, these ratios are significantly different for the two fallout sources with values of 0.029 ± 0.003 (Hardy et al., 1973; Hodge et al., 1996; Kelley et al., 1999) and 0.009 (Muramatsu et al., 2000) for the global and Chernobyl fallout, respectively.

Excess Lead-210 (^{210}Pb$_{ex}$) could also be used to overcome these restrictions in the Swiss alpine areas or more generally in areas which have been affected by heterogeneous ^{137}Cs fallout. In contrast to ^{137}Cs and $^{239+240}$Pu, ^{210}Pb$_{ex}$ is a natural geogenic radioisotope ($t_{1/2}$ = 22.3 years), which origins from the decay of Radium-226 (^{226}Ra). ^{226}Ra is found in most soils and rocks and produces as its daughter short-lived gaseous Radon-222 (^{222}Rn) having a half-life of 3.8 days. Most of this ^{222}Rn decays to ^{210}Pb within the soil, producing supported ^{210}Pb that is in equilibrium with the parent ^{226}Ra. However, some of the ^{222}Rn diffuses from the soil into the atmosphere, where it rapidly decays to ^{210}Pb. This additional ^{210}Pb is deposited on the ground via precipitation and since it is not in equilibrium with the parent ^{226}Ra, it is commonly termed unsupported or excess ^{210}Pb (^{210}Pb$_{ex}$). Because of its natural origin, ^{210}Pb$_{ex}$ fallout is essentially constant through time, although seasonal and longer-term variations in ^{210}Pb$_{ex}$ concentrations in the atmospheric fallout (rain, snow and dry deposition) have been reported (Preiss et al., 1996). As supported ^{210}Pb can be subtracted from total Pb in considering the ^{226}Ra to ^{210}Pb ratios, the determination of ^{210}Pb$_{ex}$ has been used successfully worldwide for soil erosion assessment in the last decades (Porto and Walling, 2012; Gaspar et al., 2013; Porto et al., 2013; Mabit et al., 2014). However, its suitability as soil erosion tracer in permanent alpine grasslands has not yet been tested and validated.

This study aims to fill this gap by evaluating the suitability of ^{210}Pb$_{ex}$ in addition to $^{239+240}$Pu for assessing soil erosion magnitude in alpine grassland areas under three different types of management (i.e. hayfield, pasture and pasture with dwarf shrubs). Further, we hypothesise that ^{137}Cs based soil redistribution estimates can be improved, if information on the relative contribution of the global versus Chernobyl fallout is known. The latter will be determined by calculating $^{239+240}$Pu/^{137}Cs activity ratios at reference sites. The application of the three FRNs pursues the ultimate goal to assess soil redistribution rates for the alpine grassland management type hayfield, pasture and pasture with dwarf shrubs.

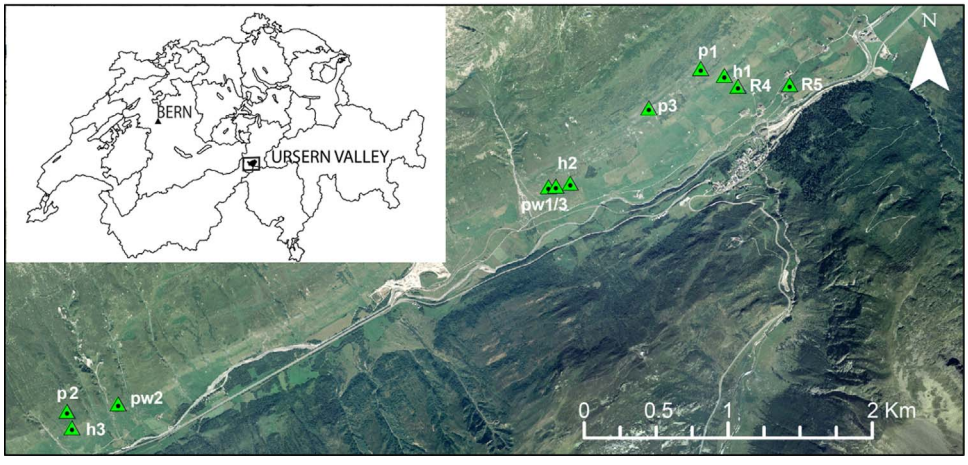

Fig. 1. Location of the 9 investigated sites (hayfields – h; pastures – p; pastures with dwarf shrubs – pw) and the two reference sites (R4, R5) in the Urseren Valley (Central Swiss Alps).

2. Materials and methods

2.1. Site description and soil sampling

As a pilot alpine study site, the Urseren Valley located in Central Switzerland (Canton Uri, Fig. 1) was selected due to the availability of ancillary data e.g. on the $^{239+240}$Pu isotopes (Alewell et al., 2014) and ^{137}Cs (Konz et al., 2012) in-situ measurements. The U-formed alpine valley extends in an E-W direction with elevations ranging between 1400 and 2500 m a.s.l. At the valley bottom (1442 m a.s.l.), average annual air temperature for the years 1950–2012 is around 3.7 ± 0.7 °C and the mean annual rainfall precipitation reaches about 1419 ± 266 mm, with approximately 30% of it falling as snow, which covers the valley from November to April (MeteoSwiss, 2013). The predominant soils are Cambisols and Podzols (anthric) based on the IUSS Working Group (2006) classification with sandy loam to loamy sand texture.

Ever since the deforestation of the valley by the Romans in the eleventh century, the vegetation cover consists of hayfields and pastured grasslands (63% of the area) that are, to a large extent, mixed or even dominated by dwarf shrubs. The proportion of forests, which protect the slopes from avalanches upslope of the main villages, represents only 1% of the surface cover. Grasslands are mainly located at slopes with median slope angles of 29° with standard deviation of 10°. These slopes are susceptible to snow avalanches and snow-gliding. These processes are besides rainfall erosivity a major trigger for soil removal (Meusburger et al., 2014). In the last decades, land use intensity increased on the lower slopes (where the study sites are located) and decreased in the higher, more remote areas (Meusburger and Alewell, 2008).

In summer 2014, a total of 82 soil profiles (> 40 cm or until reaching the bedrock) were collected with a soil corer of 59 mm diameter and 90 cm in length (Giddings Machine Company, Windsor, CO, USA). We selected nine erosional sites (at slopes near the valley bottom 1469–1616 m a.s.l) and two reference sites for our study (1476 and 1514 m a.s.l.). The erosional sites were selected to have similar topographic characteristics (planar south facing slopes of 35–39° with a natural flow barrier above) as well as soil properties (sandy loam to silt loam with a soil organic matter content of 11–13%), but with differing land use management. For a comprehensive list of site parameters, the reader is referred to Konz et al. (2009). The grassland management is subdivided into three categories: hayfields (h1-3), pastures (p1-3) and pastures with dwarf shrubs (pw1-3; Fig. 1). Dwarf shrubs are abundant in alpine grasslands and are expected to have different erosion susceptibility due to differences in root morphology but also because of different interaction with rainfall erosivity and surface runoff. At each site, we collected 9 cores, of which 3 were sectioned into 2 cm depth increments and subsequently composited. The remaining 6 cores were sectioned in 2 parts 0–10 cm and 10 to > 40 cm. The previous will yield a detailed representative depth profile for each land use and the latter will allow for an assessment of the small scale variability at each site. For $^{239+240}$Pu only a subset of these samples (n = 21) has been measured (Table 1).

A major challenge was the selection of suitable reference sites. In previous samplings, we considered 6 potential reference sites of which some showed a higher stability and reliability assessed with an resampling approach (Arata et al., 2017). For the two sites considered suitable according to this approach (R4 and R5), we collected 5 cores that were sectioned in 1 cm depth increments until the depth of 5 cm and from there on in 3 cm increments. The depth increments of the five individual cores were mixed per corresponding depth to generate a representative composite depth profile of ^{210}Pb$_{ex}$ and ^{137}Cs. In order to assess the small-scale variability, 5 additional cores were collected in close vicinity and sectioned in two parts (0–10 cm and 10 to > 40 cm). For $^{239+240}$Pu we used reference data of two different profiles (each a composite of three cores; sectioned in 3 cm increments) at R4 and R5. The $^{239+240}$Pu reference profiles we sectioned at different depth increments and could therefore not be used to calculate the $^{239+240}$Pu/^{137}Cs activity ratios. For this purpose we used Pu and Cs data of six reference sites with 3 cm increments of Alewell et al. (2014).

2.2. Radioisotopic analysis

The determinations of ^{210}Pb$_{ex}$ in the soil samples were carried out using two high resolution HPGe gamma detectors at the Department of Agraria at the University Mediterranea of Reggio Calabria, Italy. The samples were sealed for 21 days prior to assay for achieving equilibrium between ^{226}Ra and its daughter ^{222}Rn. Measurements were performed for total ^{210}Pb and ^{226}Ra (via ^{214}Pb) activities and counting times were ca. 80,000 s providing a precision of ca. ± 10% at the 95% level of confidence. The relative uncertainty associated with the determination of ^{210}Pb$_{ex}$ derived by subtracting the two measurements was around ± 14% at the 95% level of confidence. The detectors were calibrated using customized standards comprising sediment of a similar grain size composition and density to the measured samples to which known amounts of certified multi-element standard (including ^{210}Pb) had been added prior to homogenization. The standards were presented to the detectors in containers of identical geometry to those used for samples collected for the study. A correction factor of 0.78 was used to take account of exhalation loss of unsupported (also termed excess) ^{210}Pb when calculating the ^{226}Ra supported ^{210}Pb activity. This correction factor was based on the average ratio of the measured total ^{210}Pb and ^{226}Ra concentrations for samples collected from the lower part of the soil profile, where fallout ^{210}Pb was assumed to be absent (Graustein and Turekian, 1986; Wallbrink and Murray, 1996).

The measurement of Plutonium isotopes (239 + 240Pu) activity was performed at the Northern Arizona University using a Thermo X Series II quadrupole ICP-MS. The ICP-MS instrument was equipped with a high-efficiency desolvating sample introduction system (APEX HF, ESI Scientific, Omaha, NE, USA). A detection limit of 0.1 Bq kg-1 for 239 + 240Pu was obtained for samples of nominal 1 g of dry-ashed material and for 239 + 240Pu activities above 1 Bq kg-1, the measurement error was 1–3%. Prior to mass spectrometry analysis, the samples were dry-ashed and spiked with 0.005 Bq of a 242Pu yield tracer (obtained as a licensed solution from NIST). Pu was leached with 16 M nitric acid overnight at 80 °C, and was subsequently separated from the leach solution using a Pu-selective TEVA resin (Ketterer et al., 2011). The masses of 239Pu and 240Pu present in the sample were determined by isotope dilution calculations and then converted into the summed 239 + 240Pu activity.(Meusburger et al., 2016). For more details regarding the pros and cons of 239 + 240Pu analytics, the reader is referred to Alewell et al. (2017).

2.3. Conversion of FRN inventories to soil erosion rates

The mass activities (Bq kg^{-1}) of the FRNs were converted into areal activities also termed inventories (Bq m^{-2}) with the measured mass depth of fine soil material (kg m^{-2} sampling depth^{-1}). Subsequently, the inventories were derived into soil redistribution rates using the Diffusion and Migration Model (DMM) (Walling et al., 2002, 2014) and Modelling Deposition and Erosion rates with RadioNuclides (MODERN; (Arata et al., 2016a, 2016b)).

MODERN returns soil erosion and deposition rates in terms of thickness of the soil layer affected by soil redistribution processes. To estimate the thickness of soil losses/gains, MODERN aligns the total inventory of the sampling site to the depth profile of the reference site. The point of intersection along the soil profile represents the solution of the model (Arata et al., 2016a, 2016b). For ^{210}Pb$_{ex}$, a time span of 100 years is considered to convert the soil redistribution depth (cm) into soil erosion rates (Mg ha^{-1} yr^{-1}), because only around 4% of the original deposition will remain longer than 100 years due to radioactive decay. It is assumed that the contribution of previous ^{210}Pb$_{ex}$ deposit older

Table 1
Soil sampling design, mean inventory values (Bq m^{-2}) and heterogeneity of ^{137}Cs, $^{210}Pb_{ex}$ and $^{239+240}Pu$ and inventories as coefficient of variation (CV) in% at reference sites in the Urseren Valley (Switzerland). $^{239+240}Pu$ reference data from Arata et al. (2017). DW = dwarf shrubs. Numbers in brackets give replicates.

	^{137}Cs	$^{210}Pb_{ex}$	$^{239+240}Pu$
Number of sampling sites	9 (44)	9 (44)	5 (21)
Hayfields	h1 (2), h2 (5), h3 (6)	h1 (2), h2 (5), h3 (6)	h2 (3), h3 (3)
Pastures	p1(1), p2 (6), p3 (6)	p1(1), p2 (6), p3 (6)	p2 (3), p3 (3)
Pastures with DW	pw1 (6), pw2 (6), pw3 (6)	pw1 (6), pw2 (6), pw3 (6)	pw1 (3), pw2 (3), pw3 (3)
Hayfield inventory (± Stdev)	2371 ± 431		33 ± 5
Pasture inventory (± Stdev)	1985 ± 91		34 ± 18
Pasture DW inventory (± Stdev)	3096 ± 688		44 ± 8
Mean reference inventory	7421	8068	67
CV for reference sites	32	32	13
Number of reference cores	5 & one composite of 5 cores for R4 and R5	5 & one composite of 5 cores for R4 and R5	Composites of 3 cores for R4 and R5
Soil redistribution rates (Mg $ha^{-1}yr^{-1}$)			
Conversion model	DMM	MODERN	MODERN
Mean hayfield (min-max)	−5.7 (−7.4 to −3.4)	−5.2 (−11.8 to 3.4)	−5.6 (−9.2 to −3.6)
Mean pasture (min- max)	−6.7 (−8.4 to −4.7)	−9.8 (−25.2 to −2.9)	−7.0 (−21.4 to −0.3)
Mean pasture DW (min- max)	−5.2 (−9.4 to 0.5)	−4.5 (−11.5 to 0.3)	−3.3 (−8.2 to −0.2)
Mean of all grassland sites	−5.8	−6.3	−5.1

than one century is insignificant (Walling et al., 2002). The second assumption includes that the erosional sites and reference site received the same annual $^{210}Pb_{ex}$ fallout.

The DMM considers the varying input flux over the year and the slow downward movement of the FRN into the soil profile (Walling et al., 2014). The varying input flux is particularly advantageous in the context of ^{137}Cs, since it allows considering the relative fallout contributions originating from the global and the Chernobyl fallout. For the conversion of $^{210}Pb_{ex}$ inventories to soil erosion rates an adaptation of the DMM can be applied for uncultivated sites making two key assumptions (Walling et al., 2011). The first assumption is like for MODERN related to the time period of 100 years considered for the conversion. Secondly, it is assumed that the annual $^{210}Pb_{ex}$ fallout remains constant through time. Particle size selectivity during the erosion, transport and deposition processes may greatly alter the outcome of conversion models. But in this study, we did not implement a particle size correction factor, because erosion plot measurements at our pastured sites did not highlight a significant change in particle size composition between the source soils and the collected sediments (Konz et al., 2012).

3. Results and discussion

3.1. Establishment of FRN baseline inventories and shape of the depth profiles

$^{210}Pb_{ex}$, ^{137}Cs and $^{239+240}Pu$ activities for the reference sites decreased exponentially following a polynomial distribution with depth (Fig. 2). On average, 44% of the $^{210}Pb_{ex}$, 34% of the ^{137}Cs and 25% of the $^{239+240}Pu$ activity was present in the top 3 cm and 90% of the $^{210}Pb_{ex}$, 96% of both the ^{137}Cs and $^{239+240}Pu$ activity was concentrated in the upper 15 cm. The total inventory of the reference sites R5 is for all FRNs lower than the R4 site. For $^{210}Pb_{ex}$, the deviation lies within the observed small scale variability (expressed as coefficient of variation) of 32%. For ^{137}Cs having the same CV of 32% and $^{239+240}Pu$ with a lower CV of 13%, the deviation lies outside this range. Taking into account the number of reference samples and the CV, the allowable error estimated according to Mabit et al. (2012) at 90% confidence level is 20% for ^{137}Cs and $^{210}Pb_{ex}$ and 10% for $^{239+240}Pu$. Further for R5, the shape of the ^{137}Cs depth distribution points towards a disturbance or more likely towards heterogeneous input of ^{137}Cs, which led us to omit the respective reference inventory of R5. Conversion to soil erosion rates has been performed using the R4 reference inventories of 8068 Bq m^{-2} for $^{210}Pb_{ex}$, 7421 Bq m^{-2} for ^{137}Cs and 67 Bq m^{-2} for $^{239+240}Pu$. For $^{210}Pb_{ex}$ and ^{137}Cs the DMM was fitted to the depth profile to determine the migration rate (V), the diffusion rate (D) and the relaxation depth (H) of V = 0.5 ($V_{Cs\text{-}137}$ = 0.5), D = 109 ($D_{Cs\text{-}137}$ = 38) and H = 5 ($H_{Cs\text{-}137}$ = 5) for $^{210}Pb_{ex}$ and ^{137}Cs, respectively.

While the ^{137}Cs inventories and the CV correspond well with the reference inventory established at 6892 ± 2199 Bq m^{-2} for a different set of 6 reference sites in the Urseren Valley, the $^{239+240}Pu$ reference inventory is with 67 Bq m^{-2} close to the lowest range of values (i.e. 83 ± 11 Bq m^{-2}) reported by Alewell et al. (2014). Because of lack of existing data, such comparison for $^{210}Pb_{ex}$ was not possible. However, the mean annual $^{210}Pb_{ex}$ fallout flux, which is well correlated with the mean annual rainfall (Beks et al., 1998; Winkler and Rosner, 2000; Baskaran, 2011), should indicate a plausible value of around 255 Bq m^{-2} yr^{-1} and confirms a higher plausibility of the elevated inventory found in R4 as compared to R5 (172 Bq m^{-2} yr^{-1}). For comparison purpose, in southern Germany, the mean annual ^{210}Pb deposition flux was estimated at 180 Bq m^{-2} yr^{-1} with a mean annual precipitation of 855 mm (Winkler and Rosner, 2000) and in central Hungary (Budapest) at 81 Bq m^{-2} yr^{-1} with a mean annual precipitation of 476 mm (Central Radioanalytical Laboratory of Food and Feed Safety Directorate, 2006).

3.2. Comparison of fallout radionuclide inventories and conversion models

At the investigated sites, atomic ratios of $^{240}Pu/^{239}Pu$ were close to the global fallout ratio of 0.18, indicating the absence of Chernobyl derived $^{239+240}Pu$.

In contrast, ^{137}Cs originates from two different sources (i.e. the global fallout having a peak fallout in 1963 and the Chernobyl NPP accident in April-May 1986). Therefore we need to know the relative proportions of these fallout events to the total inventory to estimate erosion rates with the ^{137}Cs method. To determine this proportion, we consulted available $^{239+240}Pu$ and ^{137}Cs data of six reference soil depth profiles studied by Alewell et al. (2014). The shape of the $^{239+240}Pu/^{137}Cs$ activity ratio depth profiles varies distinctly among the different reference sites. However, for all profiles, we observe an increase with soil depth indicating a higher proportion of global fallout in deeper soil layers, while in the topsoil ^{137}Cs originating from Chernobyl is predominant (Fig. 3). The predominance of the Chernobyl fallout in the topsoil is because of its more recent fallout. The peak of the bomb-derived ^{137}Cs already occurred in 1963. Consequently migration processes may have caused depletion of the ^{137}Cs content in the upper soil layers. On average, the Chernobyl contribution amounts up to 75%. This average value will be used for the conversion of ^{137}Cs inventories. Considering the greater proportions of ^{137}Cs in the topsoil, this might lead to an overestimation of low erosion rates and an underestimation of high erosion rates, respectively. The 75% estimate derived from the activity ratios is in good agreement with previous studies conducted in

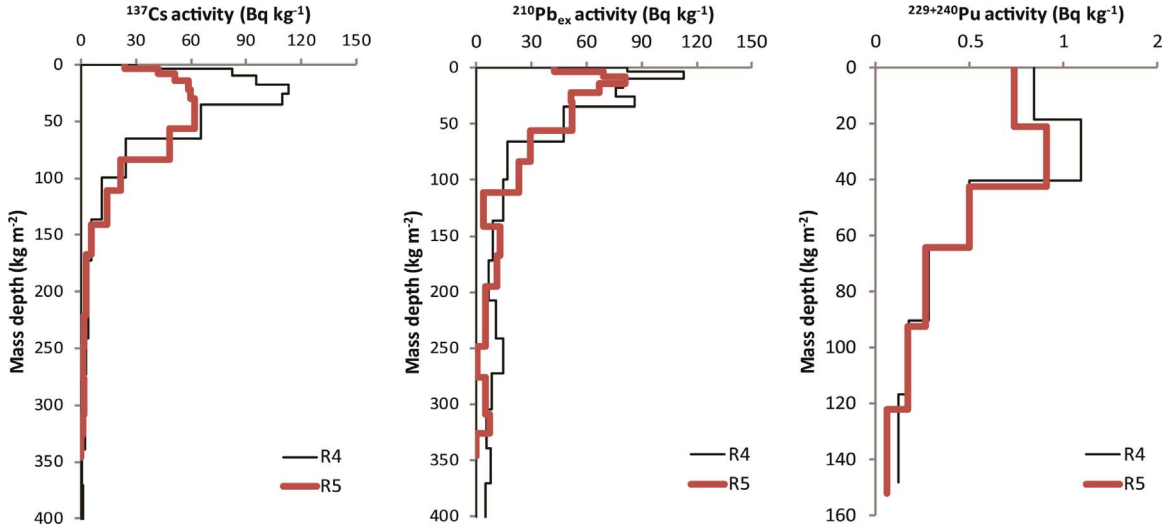

Fig. 2. ^{137}Cs, ^{210}Pb$_{ex}$ and $^{239+240}$Pu mass activity per mass-depth for the two reference depth profiles (R4 and R5).

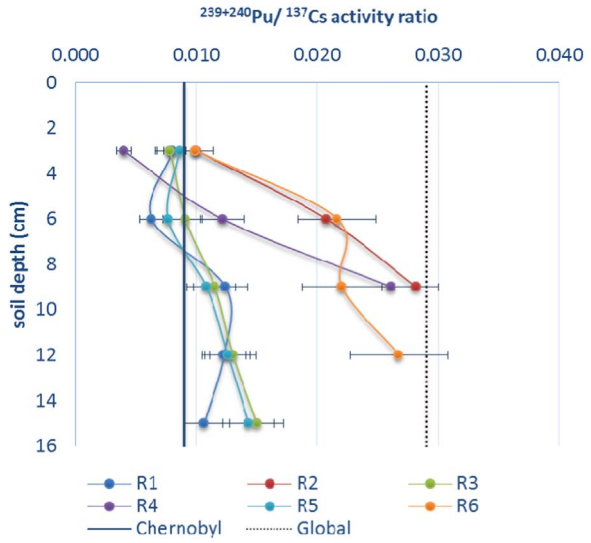

Fig. 3. $^{239+240}$Pu/^{137}Cs activity ratios with soil depth observed for six reference sites (MP1-6). The vertical black line indicates the typical isotopic ratio of the Chernobyl fallout and the vertical dashed line represents the specific ratio for the global fallout.

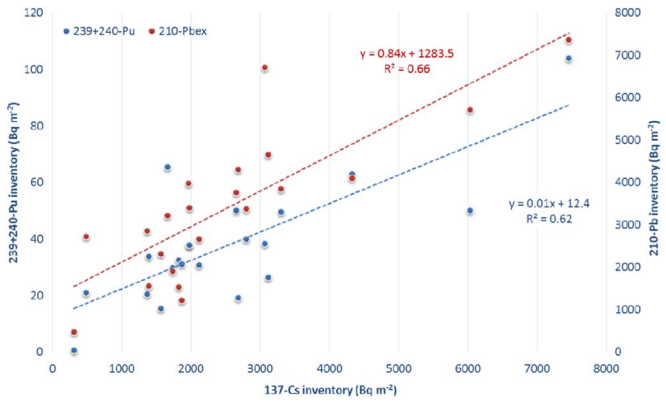

Fig. 4. Comparison of ^{210}Pb$_{ex}$ and $^{239+240}$Pu with ^{137}Cs inventories for the erosional alpine grassland sites (Urseren Valley, Switzerland).

the Swiss Alps that assumed an 80% contribution (Schaub et al., 2010; Alewell et al., 2014).

The correlations between ^{137}Cs and ^{210}Pb$_{ex}$ inventories ($p < 0.0001$, adjusted $R^2 = 0.66$; Fig. 4) as well as between ^{137}Cs and $^{239+240}$Pu inventories ($p < 0.0001$, adjusted $R^2 = 0.62$; Fig. 4) at the sampling sites are surprisingly high considering the different fallout origins. The ^{210}Pb$_{ex}$ inventories show a very high correlation close to a 1:1 relation with the ^{137}Cs inventories, with a slightly higher scattering towards the high inventories (which are closer in values to the reference inventory). The observed FRN inventories measured at the erosional/depositional sites are a result of both the initial fallout and the subsequent soil redistribution processes. For the initial fallout, a close relation between ^{210}Pb$_{ex}$ and $^{239+240}$Pu with ^{137}Cs was not expected due to the spatially heterogeneous ^{137}Cs Chernobyl fallout (Fig. 3). However, we assume that the subsequent soil loss after 1986 will affect all radionuclides equally. As such, the smaller deviation between ^{210}Pb$_{ex}$ and $^{239+240}$Pu with ^{137}Cs inventories for sites with low inventories point to the influence of erosional processes after the main ^{137}Cs fallout deposited in 1986 (Fig. 4).

We used the conversion models MODERN and DMM to convert the FRN inventories into soil redistribution rates. For our alpine sites, the DMM is most suitable for the ^{137}Cs data set, because this conversion model can account for the dual ^{137}Cs input. In implementing the DMM fitting parameters and considering a 75% ^{137}Cs Chernobyl contribution, a regression analysis yielded comparable ($p < 0.001$) and only slightly lower soil redistribution rates for ^{137}Cs as compared to ^{210}Pb$_{ex}$ estimates ($y = 1.12x$; $R^2 = 0.65$; y and x soil redistribution rates assessed with ^{210}Pb$_{ex}$ and ^{137}Cs, respectively). The above discussed deviations between ^{137}Cs and ^{210}Pb$_{ex}$ for small inventory changes and thus small soil redistribution rates are also visible here (Fig. 5).

Mean MODERN based ^{210}Pb$_{ex}$ soil redistribution estimates are comparable to the DMM results for ^{210}Pb$_{ex}$, but include a wider range of soil redistribution rates (Fig. 6). The deviation between the two conversion models is significant for sites, which experienced large inventories changes. The latter is because MODERN does not consider the continuous input of ^{210}Pb$_{ex}$ over time during the soil redistribution process. For $^{239+240}$Pu, MODERN and the DMM agreed well and provided similar results ($p < 0.0001$, adjusted $R^2 = 0.84$).

3.3. Soil erosion estimates for three land use types

A comparison among the different grassland management types displays a similar ranking with respect to soil erosion susceptibility for all FRNs used (Table 1), with highest erosion rates for pastures (-6.7 ± 1.1, -9.8 ± 6.8, -7.0 ± 5.2 Mg ha^{-1} yr^{-1} for ^{137}Cs, ^{210}Pbex and $^{239+240}$Pu, respectively) followed by hayfields (-5.7 ± 4.4, -5.2 ± 1.5, -5.6 ± 2.1 Mg ha^{-1} yr^{-1}for ^{137}Cs, ^{210}Pbex and $^{239+240}$Pu, respectively), and lowest rates for pastures with dwarf shrubs

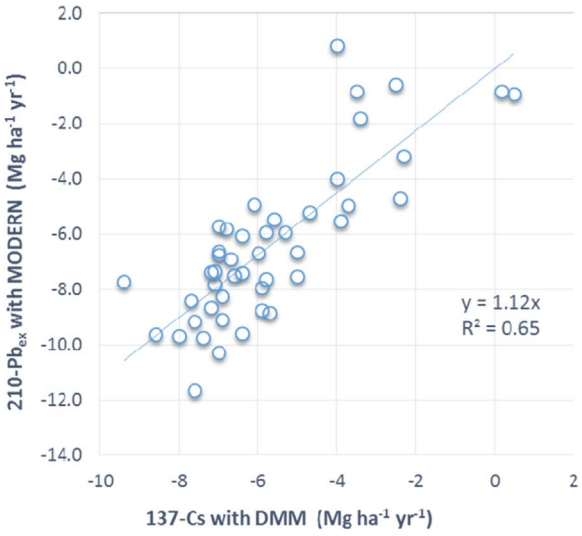

Fig. 5. Comparison of ^{137}Cs (conversion model: DMM) and ^{210}Pb$_{ex}$ (conversion model: MODERN) derived soil redistribution rates considering the ^{137}Cs Chernobyl contribution. NB: For visibility purpose, error bars that reach up to 20% have not been plotted.

(-5.2 ± 3.1, -4.5 ± 2.5, -3.3 ± 2.4 Mg ha^{-1} yr^{-1} for ^{137}Cs, ^{210}Pbex and $^{239+240}$Pu, respectively).

The standard deviation of erosion rates between the sites is particularly high for ^{210}Pb$_{ex}$. The latter does not only reflect the high initial variability of ^{210}Pb$_{ex}$ established in the reference sites, but is likely overlain by heterogeneous input at the erosional sites due to snow redistribution in winter and subsequent melting in spring. Consequently, ^{210}Pb$_{ex}$ derived erosion rates at our site might be biased towards higher estimates by the snow redistribution. However, considering the overall good agreement of the inventories between the different FRNs (Fig. 4), this effect is likely of minor importance.

Independent of the FRN used, there is agreement in the mean erosion rate over all sites and per grassland type, however the range of values observed at individual sampling points varies considerably between the applied FRNs. The deviations in the range of soil redistribution rates at individual sites are potentially caused by one or more of the following reasons. Firstly, the intrinsically small variability, which is further enhanced through the small scale soil redistribution patterns and trampling of grazing animals. Secondly, by the differences between the conversion models used. The DMM generally smooths the extreme values (Fig. 6). For ^{137}Cs and ^{210}Pb$_{ex}$, exactly the same sample volumes were measured. However, for $^{239+240}$Pu the different sample volume may play a role as only a subsample of 2–3 g (< 10% of the total) was extracted for the Pu analysis. As such, special care is required to obtain a representative sub-sample. Thirdly, preferential removal of fine soil particles – that contain varying proportions of the total inventory depending the tested FRN – need to be expected in areas, where water erosion is predominant (Meusburger et al., 2016). Finally, the different time frame that is captured by the different radionuclides needs to be considered. Even though ^{210}Pb$_{ex}$ inventories are influenced by the last 100 years of fallout deposition, ^{210}Pb$_{ex}$ is nevertheless in general more sensitive to recent erosion changes (20–30 years) due to its origin and shorter half-life and as well to its higher concentration at the soil surface when compared to the other two tested FRNs (Fig. 2). ^{137}Cs is expected to cover an intermediate time span at our sites due to the predominant Chernobyl input, while $^{239+240}$Pu is reporting about the soil redistribution status since the mid-1960s.

Regarding the three different grassland management types studied, the soil redistribution rates differ only significantly (Kruskal-Wallis test, $p < 0.05$) between pastures and pastures with dwarf shrubs. The dwarf shrub cover may be more effective in shielding the soil from rain splash. Moreover, the shrubs may also act as physical barriers not only for snowmelt- and surface runoff, but also for snow movement and its associated sediment (Konz et al., 2012; Meusburger et al., 2014).

The selected steep sites are expected to represent grassland sites with elevated soil erosion risk. Nonetheless, comparable management at slopes between 30 and 40° can be found in one third of the catchment.

Different measurements across the Alps demonstrate that an intact vegetation cover prevents almost all soil loss by water erosion (Martin et al., 2010; Schindler Wildhaber et al., 2012). However, erosion studies conducted at grassland plots with clear signs of degradation (reduced vegetation cover), established even mean erosion rates as high as 20 Mg ha^{-1}yr^{-1} during a six-year measurement period on flysch and molasse material in the Allgaeu Alps (Frankenberg et al., 1995). In the Bavarian Alps (Limestone Alps), Felix and Johannes (1995) found erosion rates of 4.4 Mg ha^{-1}yr^{-1} (during a two-year measurement period) on a pastured grassland test plot with a fractional vegetation cover of 66%. In another area of the Bavarian Alps, Ammer et al. (1995) measured soil erosion rates of approximately 2–9 Mg ha^{-1}yr^{-1} (during a five-year measurement period) after clear cutting of the small forested catchments, which geologically belong to the flysch and limestone formations. A review of erosion measurements on marls in the French Alps reported erosion rates of 1.4–33 mm yr^{-1} (Descroix and Mathys, 2003).

In addition, to potentially high erosion rates caused by disturbed vegetation cover, locally we can observe very high erosion rates due to snow movement (avalanches and snow gliding), which are not yet considered in the existing soil erosion risk modelling (Jomelli and Bertran, 2001; Ceaglio et al., 2012; Korup and Rixen, 2014; Meusburger et al., 2014).

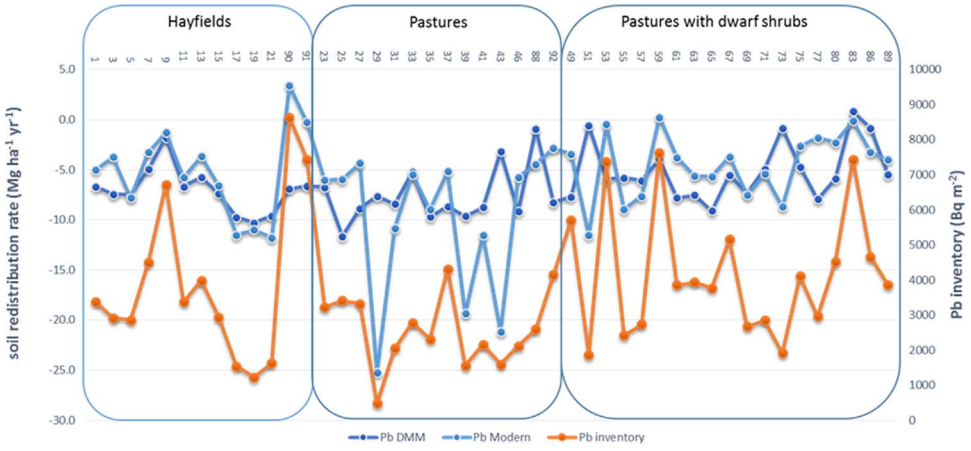

Fig. 6. ^{210}Pb$_{ex}$ derived soil redistribution estimates with the two different conversion models (DMM and MODERN). The numbers on the x-axis refer to the sample ID. NB: For visibility purpose, error bars that reach up to 20% have not been plotted.

4. Conclusion

Three FRNs have been used and combined to assess soil redistribution on three alpine grasslands. Even though $^{239+240}$Pu seems the most promising tracer in terms of measurement uncertainty and small scale variability (CV of 13%), ^{210}Pb$_{ex}$ produced nevertheless comparable results. ^{210}Pb$_{ex}$ exhibit a slightly wider range of erosion rates which seemed plausible to pattern the recent changes in soil redistribution dynamic, as such we consider both, $^{239+240}$Pu as well as ^{210}Pb$_{ex}$ suitable soil redistribution tracers at our alpine grassland sites (Urseren Valley, Central Switzerland). $^{239+240}$Pu further allowed for an assessment of the contribution of the ^{137}Cs Chernobyl fallout that helped to improve the ^{137}Cs based soil redistribution estimates.

The FRN based soil redistribution estimates at the selected 9 steep (35–38°), temporally scarcely covered (due to trampling, grazing, haying and snow melt and snow abrasion) grassland sites exhibited mean soil loss above 5 Mg ha^{-1} yr^{-1} (ranging from maximal erosion rates of −25.2 Mg ha^{-1} yr^{-1} to maximum deposition rates of +3.4 Mg ha^{-1} yr^{-1}) with a considerable small scale variably. Even though the selected sites can be considered as “hotspots” of soil erosion, it underscores the fact that compared to European arable land, too little attention has been paid to the quantification of soil erosion affecting managed mountain and alpine areas. Taking into account soil production rates in the Swiss Central Alps of 0.4–1.8 Mg ha^{-1} yr^{-1} (Norton et al., 2010), it also implies that land use at the investigated sites is not sustainable. All FRNs indicated highest soil loss for pastures, followed by hayfield and lowest for pastures with dwarf-shrubs. However, a significant difference (i.e. $p < 0.05$) in soil loss was only observed between pastures and pastures with dwarf-shrubs. In scenarios of intensifying land use of alpine grasslands entailing a decline of pastures with dwarf-shrubs, an increase of erosion rates is likely. However, alpine grasslands have been used by humans for about 5000 years (Bätzing, 2005) and increased soil erosion might be buffered, if sustainable management and maintenance efforts are reinforced in parallel to land use intensification.

Acknowledgements

The authors would like to thank Simon Tresch, Alexandra Bürge and Axel Birkholz for support during field work and Dr. Michael E. Ketterer (Chemistry Department, Metropolitan State University of Denver, Colorado, USA) for the $^{239+240}$Pu measurements. The study has been performed within the International Atomic Energy Agency Coordinated Research Project D1.50.17 on “*Nuclear techniques for a better understanding of the impact of climate change on soil erosion in upland agroecosystems*”.

References

Alewell, C., Meusburger, K., Brodbeck, M., Banninger, D., 2008. Methods to describe and predict soil erosion in mountain regions. Landsc. Urban Plan. 88, 46–53.
Alewell, C., Meusburger, K., Juretzko, G., Mabit, L., Ketterer, M., 2014. Suitability of $^{239+240}$Pu as a tracer for soil erosion in alpine grasslands. Chemosphere 103, 274–280.
Alewell, C., Pitois, A., Meusburger, K., Ketterer, M., Mabit, L., 2017. $^{239+240}$Pu from “contaminant” to soil erosion tracer: where do we stand? Earth-Sci. Rev. 172, 107–123.
Ammer, U., Breitsameter, J., Zander, J., 1995. Contribution of mountain forests towards the prevention of surface runoff and soil-erosion. Forstwiss. Cent. 114, 232–249.
Arata, L., Alewell, C., Frenkel, E., A'Campo-Neuen, A., Iurian, A.-R., Ketterer, M.E., Mabit, L., Meusburger, K., 2016a. Modelling Deposition and Erosion rates with RadioNuclides (MODERN) – Part 2: a comparison of different models to convert $^{239+240}$Pu inventories into soil redistribution rates at unploughed sites. J. Environ. Radioact. 162–163, 97–106.
Arata, L., Meusburger, K., Frenkel, E., A'Campo-Neuen, A., Iurian, A.-R., Ketterer, M.E., Mabit, L., Alewell, C., 2016b. Modelling Deposition and Erosion rates with RadioNuclides (MODERN) – Part 1: a new conversion model to derive soil redistribution rates from inventories of fallout radionuclides. J. Environ. Radioact. 162–163, 45–55.
Arata, L., Meusburger, K., Bürge, A., Zehringer, M., Ketterer, M.E., Mabit, L., Alewell, C., 2017. Decision support for the selection of reference sites using 137Cs as a soil erosion tracer. SOIL 3, 113–122.
Baskaran, M., 2011. Po-210 and Pb-210 as atmospheric tracers and global atmospheric Pb-210 fallout: a Review. J. Environ. Radioact. 102, 500–513.
Bätzing, W., 2005. Die Alpen: Geschichte und Zukunft einer europäischen Kulturlandschaft. - München.
Beks, J.P., Eisma, D., van der Plicht, J., 1998. A record of atmospheric Pb-210 deposition in The Netherlands. Sci. Total Environ. 222, 35–44.
Beniston, M., 2003. Climatic change in mountain regions: a review of possible impacts. Clim. Change 59, 5–31.
Beniston, M., 2006. Mountain weather and climate: a general overview and a focus on climatic change in the Alps. Hydrobiologica 562, 3–16.
BFS, 2009. Landwirtschaftliche Betriebszählungen, Landwirtschaftliche Betriebs-strukturerhebungen, Neuchâtel.
Borrelli, P., Robinson, D.A., Fleischer, L.R., Lugato, L., Ballabio, C., Alewell, C., Meusburger, K., Modugno, S., Schütt, B., Ferro, V., Bagarello, V., Van Oost, K., Montanarella, L., Panagos, P. An Assessment of the Global Impact of 21st Century Land Use Change on Soil Erosion.
Ceaglio, E., Meusburger, K., Freppaz, M., Zanini, E., Alewell, C., 2012. Estimation of soil redistribution rates due to snow cover related processes in a mountainous area (Valle d'Aosta, NW Italy). Hydrol. Earth Syst. Sci. 16, 517–528.
Central Radioanalytical Laboratory of Food and Feed Safety Directorate, 2006. Radioanalytical Monitoring Network of Ministry of Agriculture and Rural Development, Central Radioanalytical Laboratory of Food Feed Safety Directorate - Hungarian Agricultural Authority.
Descroix, L., Mathys, N., 2003. Processes, spatio-temporal factors and measurements of current erosion in the French Southern Alps: a review. Earth Surf. Process. Landf. 28, 993–1011.
F. Zapata, 2002. Handbook for the Assessment of Soil Erosion and Sedimentation. Dordrecht.
Felix, R., Johannes, B., 1995. Research into soil erosion on test-plots in calcareous high mountains. Mitt. Der Osterreichischen Geogr. Ges. 137, 76–92.
Fischer, G., Hizsnyik, E., Prieler, S., Wiberg, D., 2011. Scarcity and Abundance of Land Resources: Competing Uses and the Shrinking Land Resource Base. FAO, Rome, Italy.
Frankenberg, P., Geier, B., Proswitz, E., Schutz, J., Seeling, S., 1995. Investigations on soil-erosion and solid matter transport in the Gunzesrieder valley Oberallgäu. Forstwiss. Cent. 114, 214–231.
Gaspar, L., Navas, A., Machin, J., Walling, D.E., 2013. Using Pb-210(ex) measurements to quantify soil redistribution along two complex toposequences in Mediterranean agroecosystems, northern Spain. Soil Tillage Res. 130, 81–90.
Golosov, V.N., Markelov, M.V., Belyaev, V.R., Zhukova, O.M., 2008. Problems in determining spatial inhomogeneity of Cs-137 fallout for estimating rates of erosion-accumulative processes. Russ. Meteorol. Hydrol. 33, 217–227.
Golosov, V.N., Belyaev, V.R., Markelov, M.V., 2013. Application of Chernobyl-derived 137Cs fallout for sediment redistribution studies: lessons from European Russia. Hydrol. Process. 27, 781–794.
Graustein, W.C., Turekian, K.K., 1986. Pb-210 and Cs-137 in air and soils measure the rate and vertical profile of aerosol scavening. J. Geophys. Res.-Atmos. 91, 14355–14366.
Hardy, E.P., Krey, P.W., Volchok, H.L., 1973. Global inventory and distribution of fallout Plutonium. Nature 241, 444–445.
Haugen, L.E., 1991. Small-scale variation in deposition of radiocesium from the Chernobyl fallout on cultivated grasslands in Norway. Norway 465–468.
Hodge, V., Smith, C., Whiting, J., 1996. Radiocesium and plutonium: still together in "background" soils after more than thirty years. Chemosphere 32, 2067–2075.
IUSS, 2006. International Union of Soil Science, Tech. Rep.,World Reference Base for Soil Resources, FAO, Rom.
Jomelli, V., Bertran, P., 2001. Wet snow avalanche deposits in the French Alps: structure and sedimentology. Geogr. Ann. Ser. A-Phys. Geogr. 83A, 15–28.
Kelley, J.M., Bond, L.A., Beasley, T.M., 1999. Global distribution of Pu isotopes and 237Np. Sci. Total Environ. 237–238, 483–500.
Ketterer, M.E., Zheng, J., Yamada, M., 2011. Applications of Transuranics as Tracers and Chronometers in the Environment. Springer-Verlag, Berlin, Berlin.
Koning, N.B.J., Van Ittersum, M.K., Becx, G.A., Van Boekel, M.A.J.S., Brandenburg, W.A., Van Den Broek, J.A., Goudriaan, J., Van Hofwegen, G., Jongeneel, R.A., Schiere, J.B., Smies, M.:, 2008. Long-term global availability of food: continued abundance or new scarcity? NJAS - Wagening. J. Life Sci. 55, 229–292.
Konz, N., Schaub, M., Prasuhn, V., Bänninger, D., Alewell, C., 2009. Cesium-137-based erosion-rate determination of a steep mountainous region. J. Plant Nutr. Soil Sci. 172, 615–622.
Konz, N., Prasuhn, V., Alewell, C., 2012. On the measurement of alpine soil erosion. CATENA 91, 63–71.
Korup, O., Rixen, C., 2014. Soil erosion and organic carbon export by wet snow avalanches. Cryosphere Discuss. 8, 1–19.
Lasanta, T., Arnáez, J., Pascual, N., Ruiz-Flaño, P., Errea, M.P., Lana-Renault, N., 2017. Space–time process and drivers of land abandonment in (Part 3). Eur. CATENA 149, 810–823.
Lettner, H., Bossew, P., Hubmer, A.K., 1999. Spatial variability of fallout Caesium-137 in Austrian alpine regions. J. Environ. Radioact. 47, 71–82.
Mabit, L., Benmansour, M., Walling, D.E., 2008. Comparative advantages and limitations of the fallout radionuclides ^{137}Cs, ^{210}Pb$_{ex}$ and ^{7}Be for assessing soil erosion and sedimentation. J. Environ. Radioact. 99, 1799–1807.
Mabit, L., Chhem-Kieth, S., Toloza, A., Vanwalleghem, T., Bernard, C., Amate, J.I., de Molina, M.G., Gomez, J.A., 2012. Radioisotopic and physicochemical background indicators to assess soil degradation affecting olive orchards in southern Spain. Agric. Ecosyst. Environ. 159, 70–80.
Mabit, L., Meusburger, K., Fulajtar, E., Alewell, C., 2013. The usefulness of 137Cs as a tracer for soil erosion assessment: a critical reply to parsons and foster (2011). Earth-

Sci. Rev. 137, 300–307.
Mabit, L., Benmansour, M., Abril, J.M., Walling, D.E., Meusburger, K., Iurian, A.R., Bernard, C., Tarján, S., Owens, P.N., Blake, W.H., Alewell, C., 2014. Fallout $^{210}Pb_{ex}$ as a soil and sediment tracer in catchment sediment budget investigations: a review. Earth-Sci. Rev. 138, 335–351.
Martin, C., Pohl, M., Alewell, C., Korner, C., Rixen, C., 2010. Interrill erosion at disturbed alpine sites: effects of plant functional diversity and vegetation cover. Basic Appl. Ecol. 11, 619–626.
MeteoSwiss, 2013. Federal Office of Meteorology and Climatology MeteoSwiss.
Meusburger, K., Alewell, C., 2008. Impacts of anthropogenic and environmental factors on the occurrence of shallow landslides in an alpine catchment (Urseren Valley, Switzerland). Nat. Hazard Earth Syst. 8, 509–520.
Meusburger, K., Konz, N., Schaub, M., Alewell, C., 2010. Soil erosion modelled with USLE and PESERA using QuickBird derived vegetation parameters in an alpine catchment. Int. J. Appl. Earth Obs. Geoinf. 12, 208–215.
Meusburger, K., Steel, A., Panagos, P., Montanarella, L., Alewell, C., 2012. Spatial and temporal variability of rainfall erosivity factor for Switzerland. Hydrol. Earth Syst. Sci. 16.
Meusburger, K., Leitinger, G., Mabit, L., Mueller, M.H., Walter, A., Alewell, C., 2014. Soil erosion by snow gliding – a first quantification attempt in a sub-alpine area, Switzerland. Hydrol. Earth Syst. Sci. 18, 3763–3775.
Meusburger, K., Mabit, L., Ketterer, M., Park, J.-H., Sandor, T., Porto, P., Alewell, C., 2016. A multi-radionuclide approach to evaluate the suitability of Pu239 + 240 as soil erosion tracer. Sci. Total Environ. 566, 1489–1499.
Muramatsu, Y., Rühm, W., Yoshida, S., Tagami, K., Uchida, S., Wirth, E., 2000. Concentrations of 239Pu and 240Pu and their isotopic ratios determined by ICP-MS in soils collected from the chernobyl 30-km zone. Environ. Sci. Technol. 34, 2913–2917.
Norton, K.P., von Blanckenburg, F., Kubik, P.W., 2010. Cosmogenic nuclide-derived rates of diffusive and episodic erosion in the glacially sculpted upper Rhone Valley, Swiss Alps. Earth Surf. Process. Landf. 35, 651–662.
Panagos, P., Borrelli, P., Poesen, J., Ballabio, C., Lugato, E., Meusburger, K., Montanarella, L., Alewell, C., 2015. The new assessment of soil loss by water erosion in Europe. Environ. Sci. Policy 54, 438–447.
Porto, P., Walling, D.E., 2012. Validating the use of Cs-137 and Pb-210(ex) measurements to estimate rates of soil loss from cultivated land in southern Italy. J. Environ. Radioact. 106, 47–57.
Porto, P., Walling, D.E., Callegari, G., 2013. Using 137Cs and 210Pbex measurements to investigate the sediment budget of a small forested catchment in southern Italy. Hydrol. Process. 27, 795–806.
Preiss, N., Meliérè, M., Pourchet, M., 1996. A compilation of data on lead-210 concentration in surface air and fluxes at the air-surface and water-sediment interfaces. J. Geophys. Res. 101, 28847–28862.
Ritchie, J.C., McHenry, J.R., 1990. Application of radioactive fallout Cesium-137 for measuring soil-erosion and sediment accumulation rates and patterns – a review. J. Environ. Qual. 19, 215–233.
Schaub, M., Konz, N., Meusburger, K., Alewell, C., 2010. Application of in-situ measurement to determine 137Cs in the Swiss Alps. J. Environ. Radioact. 101, 369–376.
Schindler Wildhaber, Y., Burri, K., Alewell, C., Bänninger, D., 2012. Evaluation of a small hybrid rainfall simulator and its application to quantify water erosion on subalpine grassland. CATENA 91, 56–62.
Streifeneder, T., Ruffini, F.V., 2007. Selected aspects of the agricultural structure change in the Alps - a comparison of harmonised agristructural indicators at municipality level within the Alpine Convention area. Ber. Landwirtsch. 85, 406–440.
Wallbrink, P.J., Murray, A.S., 1996. Determining soil loss using the inventory ratio of excess lead-210 to cesium-137. Soil Sci. Soc. Am. J. 60, 1201–1208.
Walling, D.E., Zhang, Y., He, Q., 2011. Models for deriving estimates of erosion and deposition rates from fallout radionuclide (caesium-137, excess lead-210, and beryllium-7) measurements and the development of user friendly software for model implementation. In: Impact of Soil Conservation Measures on Erosion Control and Soil Quality, IAEA-TECDOC-1665, Vienna.
Walling, D.E., Zhang, Y., He, Q., 2014. Conversion models and related software. In: Guidelines for Using Fallout Radionuclides to Assess Erosion and Effectiveness of Soil Conservation Strategies, IAEA-TECDOC-1741, Vienna.
Walling, D.E., He, Q., Appleby, P.G., 2002. Conversion models for use in soil-erosion, soil-redistribution and sedimentation investigations. In: Handbook for the Assessment of Soil Erosion and Sedimentation using Environmental Radionuclides, Zapata, F. (Ed.), The Netherlands.
Winkler, R., Rosner, G., 2000. Seasonal and long-term variation of Pb-210 concentration in air, atmospheric deposition rate and total deposition velocity in south Germany. Sci. Total Environ. 263, 57–68.